

# Metallic corrosion in the polluted urban atmosphere of Hong Kong

Bo Liu · Da-Wei Wang · Hai Guo · Zhen-Hao Ling · Kalam Cheung

Received: 29 April 2014 / Accepted: 28 October 2014 / Published online: 18 November 2014  
© Springer International Publishing Switzerland 2014

**Abstract** This study aimed to explore the relationship between air pollutants, particularly acidic particles, and metallic material corrosion. An atmospheric corrosion test was carried out in spring-summer 2012 at a polluted urban site, i.e., Tung Chung in western Hong Kong. Nine types of metallic materials, namely iron, Q235 steel, 20# steel, 16Mn steel, copper, bronze, brass, aluminum, and aluminum alloy, were selected as specimens for corrosion tests. Ten sets of the nine materials were all exposed to ambient air, and then each set was collected individually after exposure to ambient air for consecutive 6, 13, 20, 27, 35, 42, 49, 56, 63, and 70 days, respectively. After the removal of the corrosion products on the surface of the exposed specimens, the corrosion rate of each material was determined. The surface structure of materials was observed using scanning electron microscopy (SEM) before and after the corrosion tests. Environmental factors including temperature, relative humidity, concentrations of gaseous pollutants, i.e., sulfur dioxide (SO<sub>2</sub>), nitrogen dioxide (NO<sub>2</sub>), carbon monoxide (CO), ozone (O<sub>3</sub>), and particulate-phase pollutants, i.e., PM<sub>2.5</sub> (FSP) and PM<sub>10</sub> (RSP), were monitored. Correlation analysis between environmental factors and corrosion rate of materials indicated that iron and carbon steel

were damaged by both gaseous pollutants (SO<sub>2</sub> and NO<sub>2</sub>) and particles. Copper and copper alloys were mainly corroded by gaseous pollutants (SO<sub>2</sub> and O<sub>3</sub>), while corrosion of aluminum and aluminum alloy was mainly attributed to NO<sub>2</sub> and particles.

**Keywords** Metallic corrosion · Acidic particles · Corrosion rate · Polluted urban atmosphere

## Introduction

Air pollution is a major environmental issue due to its adverse effects on human health and the environment (Godish 2004). In urban cities, material damage could be significant due to the high density of building structures. When combined with climatic effects, air pollution can cause substantial deterioration of outdoor materials, including construction materials, stone facades, and bronze statues (Nord et al. 2001). Previous study indicates that atmospheric corrosion could account for 50 % of the total corrosion loss (Landolt 1993). Substantial deterioration of materials caused by corrosion could lead to direct metal loss and reduction of lifetime of materials. In order to maintain the condition of materials and infrastructures, replacement or repair is often needed, which increases the economic cost.

Ambient acidic particles play a significant role in air pollution. The reported mean concentration of acidic

B. Liu · D.-W. Wang · H. Guo (✉) · Z.-H. Ling · K. Cheung  
Air Quality Studies, Department of Civil and Environmental  
Engineering, The Hong Kong Polytechnic University,  
Hong Kong, Hong Kong  
e-mail: ceguohai@polyu.edu.hk

particles usually ranged from about 100 to 2100 counts/cm<sup>3</sup>, representing 10–88 % of total outdoor ultrafine particles (i.e., particles with aerodynamic diameter less than 0.1 μm) in different seasons and at different sites (Cohen et al. 2004; Wang et al. 2012). In the last few decades, studies in the USA and Europe found that acid rain and acidic air pollution caused serious damages to old statues and monuments (Tzanis et al. 2009, 2011; Maeda et al. 2001; Hutzinger 1989; Baer et al. 1987).

Although some studies were conducted to evaluate the corrosion rates of various metals exposed to different atmospheric conditions (Upham 1967; Knotkova et al. 1995; Kucera and Fitz 1996; Mikhailov et al. 1995; Maeda et al. 2001), the linkage between air pollution and material corrosion is not clearly described despite its importance for the protection of construction materials, particularly in Hong Kong, where thousands of high-rise buildings exist in 2668 km<sup>2</sup> of developed land. To investigate the correlation between air pollution and metallic corrosion, it is essential to carry out atmospheric corrosion tests and field measurements. The atmospheric corrosion test is useful for qualitative and quantitative assessment of acid deposition by studying the rate and extent of metallic corrosion (Maeda et al. 2001), whereas field measurements of air pollutants provide necessary data for correlation analysis.

As one of the densest cities with rapid economic development in the world (6540 persons per square kilometer in 2010; <http://www.gov.hk/en/about/abouthk/factsheets/docs/population.pdf>), Hong Kong is facing more severe air pollution problem than many other cities. However, no study has been conducted to build up the correlation between acidic air pollution and metallic corrosion in Hong Kong. Therefore, there is an urgent need to understand the influence of air pollution on material corruptions in subtropical coastal Hong Kong.

In this study, nine types of metallic materials were exposed to ambient air for 6–70 days. Air pollutants, i.e., CO, NO<sub>2</sub>, SO<sub>2</sub>, O<sub>3</sub>, PM<sub>2.5</sub>, and PM<sub>10</sub>, and meteorological parameters including temperature and relative humidity were monitored using real-time instruments. Ultrafine diffusion monitor (UDM) was used to collect acidic particles in the atmosphere. The aim of this study is to explore the influence of air pollutants and meteorological parameters on material corrosion. It is expected that the findings obtained in this study will advance our knowledge on metallic corrosion in polluted urban atmosphere.

## Materials and method

### Atmospheric corrosion test

#### *Selection of materials*

Nine types of commonly used metallic materials were selected as specimens for corrosion tests. Ten sets of each type of material were prepared so that the corrosion rates of materials for different exposure periods could be evaluated. All the specimens were designed to have the same dimension, i.e., 2.0×25×50 mm (height×width×length). Table 1 lists the detailed information of the nine types of metallic materials.

#### *Ambient exposure experiments*

The atmospheric corrosion tests were undertaken at a residential site of Tung Chung (TC), which is adjacent to highway and railway lines. The site is located north of Lantau Island, about 3 km south of the Hong Kong International Airport. It is about 20 km to the southwest of the Hong Kong central urban center and 38 km northeast of Macau (Fig. 1). In addition to the influence of local emission sources such as vehicular emissions, TC is also affected by polluted continental air masses

**Table 1** Detailed information of the selected materials

Material	Composition
Iron	Fe >99.8 %
Q235 steel	C 0.18 %, Si 0.23 %, Mn 0.4 %, P 0.016 %, S 0.006 %, Al 0.034 %
20# steel	C 0.18 %, Si 0.22 %, Mn 0.4 %, P 0.008 %, S 0.005 %, Al 0.034 %
16Mn steel	C ≤0.20 %, Si ≤0.55 %, Mn 1.00–1.60 %, P ≤0.045 %, S ≤0.045 %, Nb 0.015–0.060 %, Ti 0.02–0.20 %, V 0.02–0.15 %
Copper	Cu >99.91 %
Bronze	Sn 2.0–4.0 %, Ni 0.5–1.5 %, Pb 4.0–7.0 %, Zn 6.0–9.0 %, Cu >78.5 %
Brass	Cu 60.5–63.5 %, Zn 35.77–38.77 %, Fe 0.15 %, Pb 0.08 %, Ni 0.5 %
Aluminum	Al >99.899 %
Aluminum alloy	Si 0.8–1.3 %, Cu ≤0.1 %, Mn 0.1–0.4 %, Mg 4.5–5.5 %, Zn ≤0.2 %, Ti ≤0.2 %, Fe ≤1.2 %

The number for steels refers to Chinese national standard, GB

from the highly industrialized Pearl River Delta (PRD) region of mainland China. Thus, this site is capable of monitoring air pollutants transported from the inland PRD region and is suitable for assessing their impact on local air quality and material corrosion. Generally, the requirements for atmospheric corrosion tests in this study followed ISO 8565: *Metals and alloys—atmospheric corrosion testing—general requirements* (ISO 2011). After surface cleaning and weighing, all the specimens were exposed to ambient air with rain shelter on the rooftop of a building at the site (about 20 m high). All the specimens were hanged in the air in a horizontal position so that one side was facing to the sky (defined as front side) and the other side was facing to the ground (defined as back side). It is noteworthy that front side was affected by both gas-phase and particulate-phase pollutants, whereas the back side was influenced only by gaseous pollutants. The atmospheric corrosion tests were performed from March to June 2012. Ten sets of the nine materials were all exposed to ambient air, and then each set was collected individually after exposure to ambient air for consecutive 6, 13, 20, 27, 35, 42, 49, 56, 63, and 70 days, respectively. After the exposure tests, the corrosion products on the surface of the test specimens were removed following ISO 8407: *Corrosion of metals and alloys—removal of corrosion products from corrosion test specimens* (ISO 2009). At last, the corrosion rate of the specimens was determined by ISO 9226: *Corrosion of metals and alloys—corrosivity of atmospheres—determination of corrosion rate of standard specimens for the evaluation of corrosivity* (ISO 2012). In brief, the corrosion rate was calculated as follows:

$$r_{\text{corr}} = \Delta m / (A \cdot t)$$

where  $r_{\text{corr}}$  is the corrosion rate [ $\text{g}/(\text{m}^2 \text{ h})$ ],  $\Delta m$  is the mass loss (g),  $A$  is the surface area ( $\text{m}^2$ ), and  $t$  is the exposure time (h).

#### Surface structure of specimens

Before the atmospheric corrosion tests, all the specimens were scanned using scanning electron microscope (SEM) to obtain the image of the surface structure of the pre-exposed specimens. After the atmospheric corrosion tests, the post-exposed specimens were scanned again using the SEM. Hence, a clear picture of the material degradation would be obtained. The difference between

the corrosion rate of the front side and the back side of the exposed specimens would be compared.

#### Measurements of air pollutants and meteorological parameters

Since the sampling site was an ambient air quality monitoring station of the Hong Kong Environmental Protection Department (HKEPD), the hourly data of air pollutants and meteorological parameters including sulfur dioxide ( $\text{SO}_2$ ), nitrogen oxides ( $\text{NO}_x$ ), nitrogen dioxide ( $\text{NO}_2$ ), carbon monoxide (CO), ozone ( $\text{O}_3$ ), respirable suspended particulates (RSP,  $\text{PM}_{10}$ ), fine suspended particulates (FSP,  $\text{PM}_{2.5}$ ), and temperature were directly obtained from the HKEPD Web site (<http://epic.epd.gov.hk/EPICDI/air/station>). The QA/QC procedures for the measurement data can be found at HKEPD Web site. The hourly data of relative humidity (RH) near the TC site (i.e., Hong Kong International Airport) was obtained from the Hong Kong Observatory (HKO).

#### Measurements of acidic particle concentration

During the sampling period, acidic particles in the air were simultaneously monitored using the Ultrafine Diffusion Monitor (UDM) and iron nanofilm detectors developed by us (Wang et al. 2012). The UDM was made of stainless steel with a flat and rectangular channel in 1.0 mm high, 50 mm wide, and 500 mm long. The iron nanofilm detectors were deployed at three different locations along the length of the channel. Ambient ultrafine particles were collected on the detectors inside the UDM by diffusion, and acidic particles were distinguished from nonacidic particles and quantified using atomic force microscopy (AFM). The quantification of acidic particle concentration was based on the following equations:

$$\mu = (DLW)/(Qh) \tag{1}$$

$$P = 0.910 \times \exp(-7.54\mu) + 0.531 \times \exp(-85.7\mu) + 0.0153 \times \exp(-249\mu) (\mu \geq 0.003) \tag{2}$$

$$P = 1 - 2.96 \times \mu^{2/3} + 0.4 \times \mu (\mu \leq 0.0003) \tag{3}$$

$$C = [N/(1-P)]/(Q \times t \times 60) \tag{4}$$

where  $\mu$  is the deposition parameter,  $D$  is the diffusion coefficient of the particle ( $\text{cm}^2/\text{s}$ ),  $L$  is the channel length (cm),  $W$  is the channel width (cm),  $h$  is the

channel height (cm),  $Q$  is the flow rate ( $\text{cm}^3/\text{s}$ ),  $P$  is the penetration efficiency (%),  $C$  is particle number concentration ( $\text{counts}/\text{cm}^3$ ),  $N$  is number of particles deposited on the detector, and  $t$  is UDM sampling time (min).

## Results and discussion

### Surface image of specimens

Figure 2 shows the surface structure of Q235 steel before and after exposure for 6 days. Some scratches on the surface of the unexposed specimen were found (Fig. 2a), while clear corrosion by-product was observed on the surface after 6-day exposure (Fig. 2b). Similarly, corrosion by-products were observed on the surface of iron, 16Mn steel, and 20# steel via SEM image after 6-day exposure, and the corrosion could be seen by naked eyes after 13-day exposure (images not shown here). However, no significant corrosion was found for copper, brass, and bronze even after 63-day exposure, and for aluminum and aluminum alloy after 27-day exposure (images not shown here).

On the other hand, after 70 days of continuous exposure, corrosion marks of all the exposed specimens were clearly observed by naked eyes. Figure 3a–c shows the surface structure of Q235 steel ( $\times 500$ ), brass ( $\times 1000$ ), and aluminum alloy ( $\times 1000$ ) after 70-day exposure. Corrosion by-products and damaged surface were

apparent for Q235 steel. On the surface of brass, some indentations were found, but no obvious corrosion by-product or protuberance caused by corrosion was identified. In contrast, the surface corrosion of aluminum and aluminum alloy was different from that of iron, steel, copper, and copper alloys. As shown in Fig. 3c, pitting corrosion was mainly formed on the surface of aluminum and aluminum alloy.

It is of interest to compare the degree of corrosion between the front side and the back side of the exposed specimens. Figure 4 presents the back-side surface structure of Q235 steel and aluminum alloy after 70-day exposure.

By comparison, the entire front side of Q235 steel was damaged and covered by corrosion by-products (Fig. 3a), whereas some areas on the back-side surface were not affected (Fig. 4a). As mentioned previously, the front side of the specimens was exposed to both particulate- and gas-phase pollutants and the back side was only impacted by the gas-phase pollutants. Thus, the difference shown in Fig. 4 was likely induced by particulate corrosion.

Different from iron and steel, the surface structures of both sides for exposed copper, brass, and bronze specimens were similar, i.e., some indentations were found on the surface of both sides without obvious corrosion by-products or protuberance (images can be provided upon request). The similar degree of corrosion of the both sides suggests that the role of particulate-phase



**Fig. 1** Location of the Tung Chung site and the surrounding environment

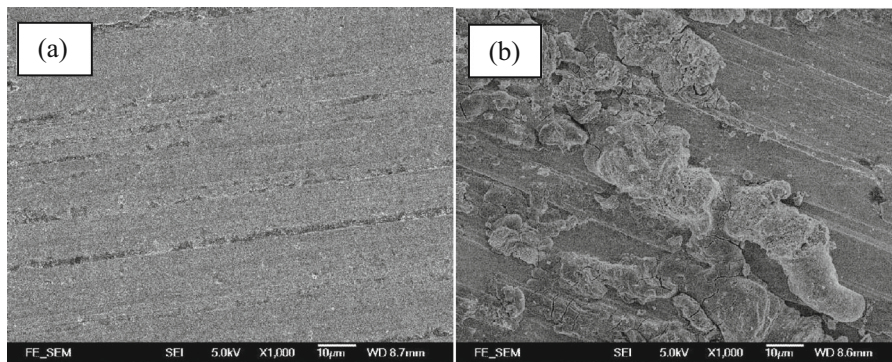


**Fig. 2** Surface structure of Q235 steel: **a** before exposure and **b** after 6-day exposure

pollutants may not be as important as gas-phase pollutants in the corrosion of copper and copper alloys.

The corrosion of aluminum and aluminum alloy showed different patterns from that of steel and copper alloys. After 35-day exposure, pitting corrosion began to appear on the front side of aluminum and aluminum alloy, while the back side was still relatively smooth. By comparing Fig. 3c with Fig. 4b, it was apparent that pitting corrosion was formed on both the front and back sides of aluminum alloy. However, it was impossible to measure the number and depth of pitting corrosion spots on both sides due to the fact that only small size of specimen could be placed into the SEM for scanning. Hence, the SEM images could not provide information on the degree of corrosion of the two sides.

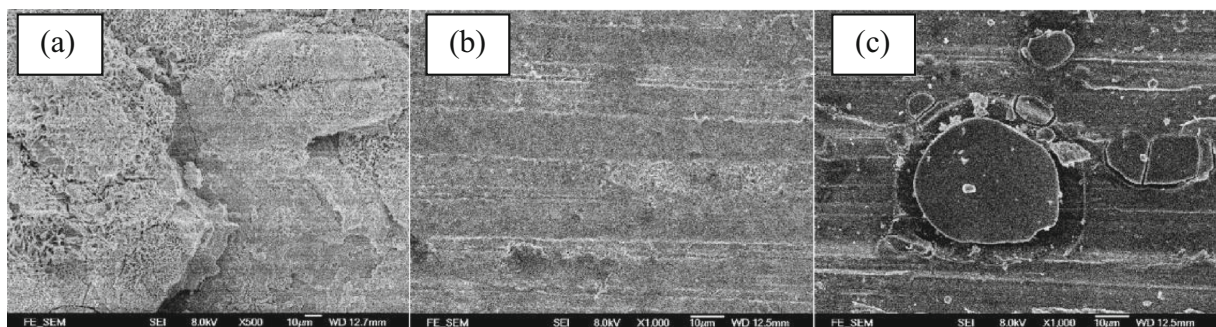
It is noteworthy that pitting corrosion formed on the surface of aluminum and aluminum alloy was only detected after 35-day exposure. This could be due to the fact that an oxidized protective film was initially formed on the surface of the aluminum alloy, preventing material from reacting with air pollutants. However, the solubility of the naturally formed oxidized film is high, and the dissolution rate of the film is greater than its rate of formation (Vargel 2004). As such, after the oxidized

film was dissolved, the surface of aluminum and aluminum alloy began to react with air pollutants.

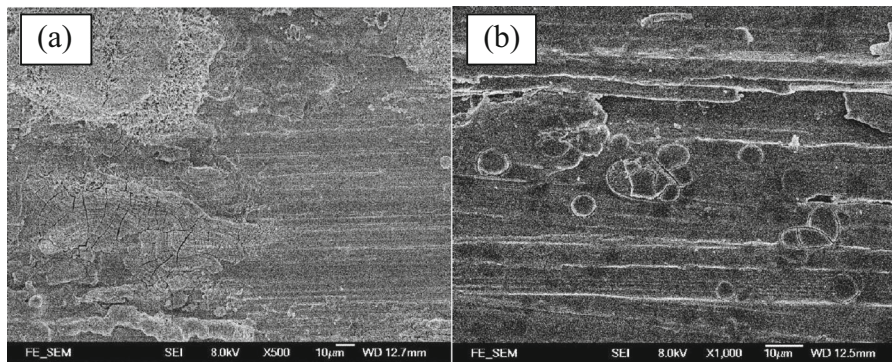
### Corrosion rate

Figure 5 illustrates the corrosion rate of each type of metallic material with exposure time. Please note, since the weight loss of copper, brass, bronze, aluminum, and aluminum alloy was too small to be measured after 6-day exposure, there were only 9 data points for each type of material in the bottom figure.

Overall, the corrosion rate of each material increased with exposure time, reached a maximum value before it decreased with time (Fig. 5). The corrosion rate of iron and steels was much higher than that of copper, copper alloys, aluminum, and aluminum alloys (*t* test, all *p* values <0.001). For iron and steels, corrosion rate of iron and 16Mn steel was generally lower than that of Q235 steel and 20# steel (*p*<0.01), but they reached the highest corrosion rate earlier (<30 days) than Q235 and 20# steels (35–42 days). On the other hand, copper/copper alloys and aluminum/aluminum alloys reached the maximum corrosion rate at the same time, i.e., around 35 days. Among the copper/copper alloys and



**Fig. 3** Surface structure of Q235 steel (a), brass (b), and aluminum alloy (c) after 70-day exposure



**Fig. 4** Back-side surface structure of Q235 steel (a) and aluminum alloy (b) after 70-day exposure

aluminum/aluminum alloy, the corrosion rate of copper and copper alloys was generally higher than that of aluminum/aluminum alloy ( $p < 0.005$ ). For the copper and copper alloys, the corrosion rate of copper was the highest while brass had the lowest corrosion rate. This was perhaps due to the interaction between copper alloys and ambient air, which rendered a passivating film on the surface of copper alloys, leading to a combination of good corrosion resistance in the atmosphere (Leidheiser 1971; Shreir 1963). Similarly, the corrosion rate of aluminum was higher than that of aluminum

alloy ( $p < 0.001$ ). The corrosion rates indicated that iron and steels were the weakest metallic materials to be corroded in the coastal urban environment, followed by copper and copper alloys, while aluminum and aluminum alloy had the lowest degree of corrosion. The different corrosion rates for different materials were attributed to the difference in metal reactivity (Shreir 1963). Iron has a high metal reactivity and can easily react with air pollutants and form corrosion by-products. Therefore, the degree of corrosion of iron and steels was more serious. The higher corrosion rate of Q235 and 20# steels than pure iron was likely due to the fact that low carbon steels are vulnerable to corrosion, because galvanic cell tends to be formed on the surface of these steels and accelerates the corrosion process. Although the metal reactivity of aluminum is better than that of iron, an oxidized protective film could be easily formed on the surface of aluminum and aluminum alloy when exposed to ambient air, which prevented the aluminum/aluminum alloy from reacting with air pollutants. Hence, the corrosion rate of aluminum and aluminum alloy was lower than that of iron, steels, copper, and copper alloy.

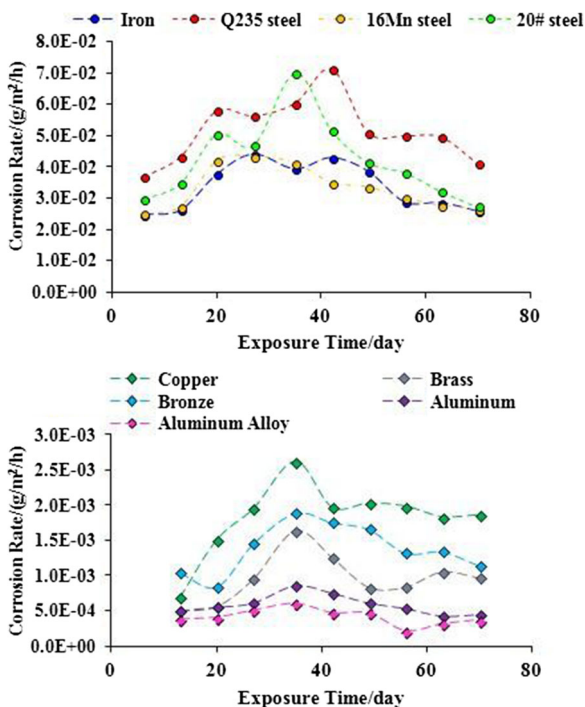


**Fig. 5** Corrosion rate of iron, Q235 steel, 16Mn steel, and 20# steel (top), and of copper, brass, bronze, aluminum, and aluminum alloy (bottom)

Influence of air pollutants and meteorological parameters on metallic corrosion

*General characteristics of air pollutants and meteorological parameters during the corrosion test periods*

Figure 6 presents the temporal variations of air pollutants and meteorological parameters in the atmospheric corrosion testing period. The average temperature and relative humidity was  $24.9 \pm 0.9$  °C and  $75.8 \pm 1.8$  % respectively, typical weather condition in spring-

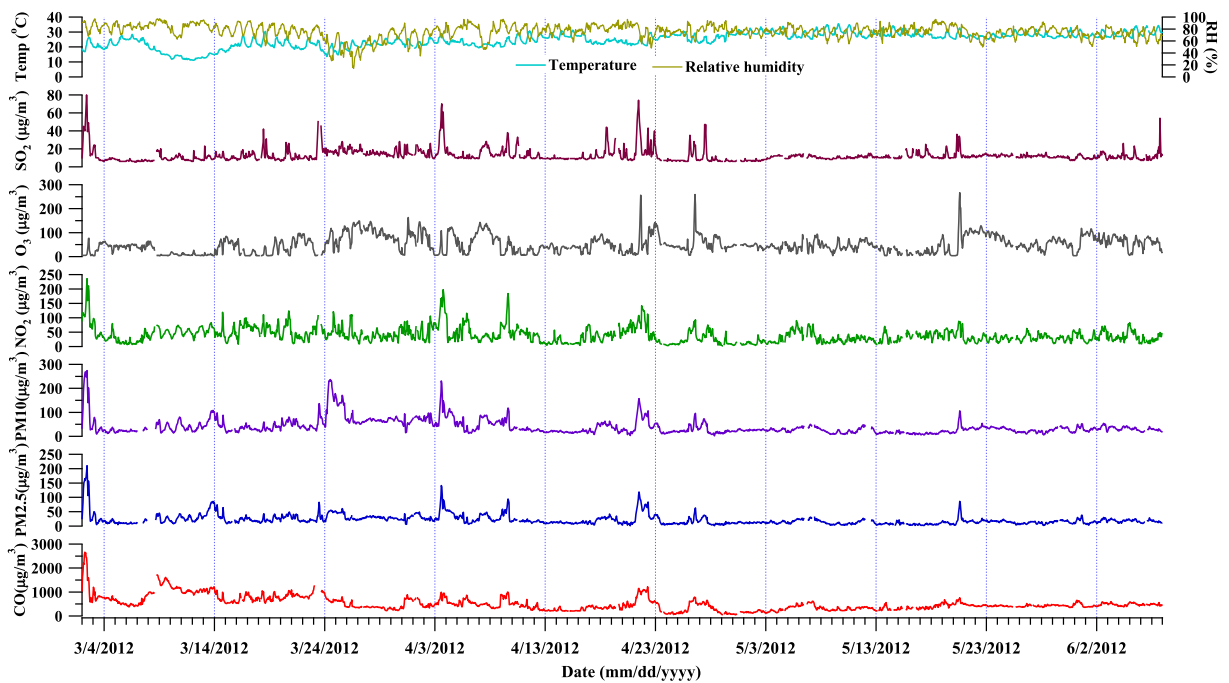


**Fig. 6** Time series of air pollutant concentrations and meteorological parameters during the exposure period

summer in subtropical Hong Kong. It was found that most air pollutant levels were higher on March 24, April 3, 22, and 27, and May 20 than on other days, which could result in the variations of metallic corrosions. Detailed discussion on the relationship between air pollutants and metallic corrosion was given in the section “Impact of air pollutants.”

To understand the source origins of air pollutants at the testing site, the correlation coefficients ( $R^2$ ) among air pollutants were calculated (Table 2). Some correlations were found between  $SO_2$  and RSP ( $R^2=0.50$ ),  $SO_2$  and FSP ( $R^2=0.60$ ),  $NO_2$  and FSP ( $R^2=0.57$ ), and RSP and FSP ( $R^2=0.75$ ), suggesting that these pollutants were from similar sources, likely from combustion

**Table 2** Squared correlation coefficient among air pollutants

Pollutant	$SO_2$	$NO_2$	CO	$O_3$	RSP	FSP
$SO_2$	1					
$NO_2$	<b>0.55</b>	1				
CO	0.15	0.49	1			
$O_3$	0.02	0.07	0.07	1		
RSP	<b>0.50</b>	0.35	0.022	0.08	1	
FSP	<b>0.60</b>	<b>0.57</b>	0.44	0.007	<b>0.75</b>	1

Values in boldface indicate significance at  $p < 0.05$

emissions. It was not surprising that no correlation was observed between  $O_3$  and other pollutants ( $R^2 < 0.08$ ), because  $O_3$  is a secondary pollutant while others are primary pollutants.

Figure 7 shows the time series of ambient acidic particle number concentration during the exposure experimental period. The number concentration of acidic particles in this period ranged from 1554 (i.e., 6-day exposure) to 2035#/cm<sup>3</sup> (i.e., 35-day exposure). The highest number concentration of acidic particles was coincident with the fact that the exposed detectors experienced most of the high pollution days such as March 24 and April 3 and 10 during the 35-day exposure period (Fig. 6). It was noteworthy that though the seventh point in Fig. 7 (i.e., 49-day exposure) covered all the high-pollution days, the number concentration of acidic particles was not the highest at this point perhaps due to the wash-out effect on rainy days, i.e., April 17 and 20 (Fig. 6).

#### Impact of relative humidity

Table 3 lists the squared correlation coefficient ( $R^2$ ) between relative humidity and corrosion rate of each material. It was found that only the corrosion rates of

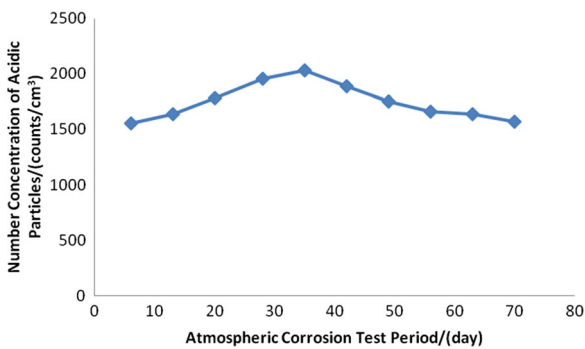


**Fig. 7** Temporal variation of number concentration of acidic particles (unit in counts/cm<sup>3</sup>, particles size <1 μm)

iron and copper had some correlations with relative humidity, while others did not.

Previous studies indicate that relative humidity plays a major role in atmospheric corrosion (Shreir 1963; Syed 2010), particularly in the corrosion of steel (Castaño et al. 2010). High relative humidity usually causes formation of water films on the surface of metal, which allows ambient acidic pollutants like SO<sub>2</sub> and NO<sub>2</sub> to dissolve in the water film and accelerates the corrosion process. However, in this study, except for copper and iron, the corrosion rates of other materials showed weak correlations with relative humidity. A possible interpretation for this is that other materials contained some elements such as aluminum, zinc, and tin, which were favorable to the formation of a protective film on the surface and subsequently prevented the materials from corrosion (Shreir 1963; Gan et al. 1991; Vargel 2004). In contrast, the protective film was unlikely formed on the surface of iron and copper, leading to good correlation between corrosion rates and relative humidity. It is noteworthy that the corrosion of copper

**Table 3** Correlation between corrosion rate of material and relative humidity

Material	R <sup>2</sup>
Iron	<b>0.41</b>
Q235 steel	0.39
16Mn steel	0.33
20# steel	0.21
Copper	<b>0.79</b>
Brass	0.41
Bronze	0.30
Aluminum	0.13
Aluminum alloy	0.09

Values in boldface indicate significance at  $p < 0.05$

seemed more related to humidity than that of iron. This is likely due to the fact that elevated relative humidity stimulates the formation rate of cuprite, the dominating phase in the corrosion patina (Wallinder and Leygraf 2001), and when the relative humidity is 75 % (the mean relative humidity in this study was 75.8 %), the water vapor content of the atmosphere becomes the controlling factor in the corrosion of copper (Leidheiser 1971). The moderate to poor association between corrosion and humidity for most materials suggested that relative humidity was not the main factor responsible for metal damage after short-term exposure.

#### Impact of air pollutants

Table 4 presents the correlation analysis between air pollutants and corrosion rates of materials. Among all the pollutants listed in Table 4, CO showed no or weak correlations with the corrosion rates of all the materials, indicating that CO had little contribution to metallic corrosion.

Clearly, the corrosion rates of iron, Q235 steel, 16Mn steel, and 20# steel correlated well with concentrations of RSP and FSP with the squared coefficient above 0.6, suggesting the importance of particulate matter on the corrosion of iron and steels. Good correlations between corrosion rate of iron, Q235 steel, 16Mn steel, and 20# steel and concentration of NO<sub>2</sub> were also found, indicating the influence of gas-phase pollutants on the corrosion. In addition, SO<sub>2</sub> showed some correlations with the corrosion rate of iron and Q235 steel. The results indicated that both gaseous pollutants and particles were responsible for the corrosion of iron, Q235 steel, 16Mn steel, and 20# steel, consistent with the fact that both sides of the Q235 steel were corroded and the damage degree of front side was more serious than that of back side (Figs. 3 and 4).

The corrosion rates of copper, brass, and bronze presented good linear relations with SO<sub>2</sub> and O<sub>3</sub>, especially for copper which had excellent correlations with SO<sub>2</sub> ( $R^2=0.94$ ) and O<sub>3</sub> ( $R^2=0.87$ ), suggesting that SO<sub>2</sub> and O<sub>3</sub> were the main pollutants for the corrosion of copper and its alloys. Aastrup et al. (2000) reported that in addition to SO<sub>2</sub>, O<sub>3</sub> is an accelerator in the atmospheric corrosion of copper. It can increase the formation rate of corrosion products such as Cu<sub>2</sub>O and CuSO<sub>4</sub>·nH<sub>2</sub>O on the surface. This might explain why the corrosion rates of copper and copper alloys had



**Table 4** Correlation between corrosion rate of material and concentration of air pollutants

Material	$R^2$					
	SO <sub>2</sub>	NO <sub>2</sub>	CO	O <sub>3</sub>	RSP	FSP
Iron	<b>0.46</b>	<b>0.45</b>	0.023	0.26	<b>0.74</b>	<b>0.63</b>
Q235 steel	<b>0.54</b>	<b>0.52</b>	0.0023	0.19	<b>0.68</b>	<b>0.64</b>
16Mn steel	0.34	<b>0.58</b>	0.14	0.14	<b>0.77</b>	<b>0.70</b>
20# steel	0.37	<b>0.59</b>	0.091	0.13	<b>0.64</b>	<b>0.67</b>
Copper	<b>0.94</b>	0.00002	0.25	<b>0.87</b>	<b>0.52</b>	0.13
Brass	<b>0.73</b>	0.029	0.12	<b>0.55</b>	0.33	0.16
Bronze	<b>0.63</b>	0.023	0.12	<b>0.49</b>	0.29	0.18
Aluminum	<b>0.45</b>	<b>0.49</b>	0.049	0.15	<b>0.57</b>	<b>0.72</b>
Aluminum alloy	0.23	<b>0.48</b>	0.15	0.089	<b>0.48</b>	<b>0.65</b>

Values in boldface indicate significance at  $p < 0.05$

significant correlations with O<sub>3</sub>. Interestingly, except for the moderate association between copper and RSP ( $R^2 = 0.52$ ), no correlations were found between the corrosion rates of copper/copper alloys and particulates (i.e., RSP and FSP). One of the possible reasons was due to the fact that unlike brass and bronze, the surface of copper did not form a protective film. Hence, the RSP could directly attack the surface of copper. In summary, the corrosion of copper and copper alloys was mainly caused by gaseous pollutants, consistent with the surface structure of the exposed materials, which showed no obvious difference between front and back sides.

The corrosion rates of aluminum and aluminum alloy were related to the concentrations of RSP and FSP, and to some extent, to the concentration of NO<sub>2</sub>. Moreover, the corrosion rate of aluminum also had some correlation with the concentration of SO<sub>2</sub>. The results of the correlation analysis indicated that corrosion of aluminum and aluminum alloy was mainly affected by particles, particularly fine particles, and gaseous NO<sub>2</sub>, consistent with the fact that both sides of the aluminum and aluminum alloy were damaged with pitting corrosion.

In summary, gaseous pollutants and particles in ambient air caused corrosion of iron, Q235 steel, 16Mn steel, 20# steel, aluminum, and aluminum alloy, while the surface damage of copper, brass, and bronze was mainly caused by gaseous pollutants in ambient air. Regardless of the corrosion mechanisms, significant material damage is usually attributed to synergetic operation of ambient gaseous pollutants such as SO<sub>2</sub>, NO<sub>x</sub>, and O<sub>3</sub> and/or particulate matters such as RSP and FSP (Maeda et al. 2001).

*Impact of number concentration of acidic particles*

The squared correlation coefficients between number concentration of acidic particles and corrosion rate of the nine materials are listed in Table 5. It can be seen that except for copper and copper alloys, corrosion of iron, steels, aluminum, and aluminum alloy correlated well with the number concentration of acidic particles ( $R^2 = 0.68 - 0.86$ ), suggesting that acidic particles were one of the factors affecting the corrosion of iron, steels, aluminum, and aluminum alloys, whereas the corrosion of copper and copper alloys was not due to the acidic particles. The results are consistent with the correlations between corrosion rate and RSP/FSP in Table 4.

**Table 5** Correlation between number concentration of acidic particles and corrosion rate of materials

Material	$R^2$
Iron	<b>0.82</b>
Q235 steel	<b>0.68</b>
16Mn steel	<b>0.80</b>
20# steel	<b>0.86</b>
Copper	0.30
Brass	0.37
Bronze	0.41
Aluminum	<b>0.79</b>
Aluminum alloy	<b>0.70</b>

Values in boldface indicate significance at  $p < 0.05$

## Conclusions

In this study, atmospheric corrosion test and field measurement were conducted to measure corrosion rate of nine materials and collect data of air pollutants and meteorological parameters. During the field measurements, the iron nanofilm detectors and UDM developed by us were employed to collect ambient acidic particles.

The advantage and innovation of this study were that multipollutants were monitored simultaneously with the corrosion test; the degree of corrosion of various metallic materials in a certain period was quantified; and the correlations between different air pollutants and material damage were characterized. In particular, the concentration of acidic particles, which could not be measured in the past, were for the first time collected and quantified using a method developed by us, leading to better understanding of the influence of acidic particles on material corrosion.

The main conclusions are drawn as follows:

1. The corrosion degree of materials followed the order of iron and steels > copper and copper alloys > aluminum and aluminum alloy.
2. Relative humidity and CO were not the main factors responsible for the damage of metallic materials after short-term exposure.
3. SO<sub>2</sub>, NO<sub>2</sub>, and particles contributed to the corrosion of iron and steels, while aluminum and aluminum alloy were damaged by NO<sub>2</sub> and fine particles. The corrosion of copper and copper alloys was mainly caused by gaseous pollutants such as SO<sub>2</sub> and O<sub>3</sub>.
4. Iron nanofilm detector and UDM were suitable to monitor ambient acidic particles. The acidic particles closely correlated with the corrosion of iron, steels, aluminum, and aluminum alloy.

**Acknowledgments** This study was supported by the internal grant of the Hong Kong Polytechnic University (A-PL40 and 87UB) and the Environment and Conservation Fund of the Hong Kong government (ECF20/2008). Special thanks go to Hong Kong Environmental Protection Department for providing the corrosion testing site.

## References

Aastrup, T., Wadsak, M., Leygraf, C., & Schreiner, M. (2000). In situ studies of the initial atmospheric corrosion of copper: influence of humidity, sulfur dioxide, ozone, and nitrogen

dioxide. *Journal of the Electrochemical Society*, 147(7), 2543–2552.

Baer, N. S., Bermabo, J. C., Lipfert, F. W., & Smythe, K. D. (1987). *Effects of acidic deposition on materials degradation. A Synthesis Report, EPRI-EA-5424*. Palo Alto: Electric Power Research Institute.

Castaño, J. G., Botero, C. A., Restrepo, A. H., Agudelo, E. A., Correa, E., & Echeverría, F. (2010). Atmospheric corrosion of carbon steel in Colombia. *Corrosion Science*, 52(1), 216–223.

Cohen, B. S., Heikkinen, M. S., Hazi, Y., Guo, H., Peters, P., & Lippmann, M. (2004). Field evaluation of nanofilm detectors for measuring acidic particles in indoor and outdoor air. *Research Report. Health Effects Institute*, 121, 1–35. discussion 37–46.

Gan, F. X., Guo, H., & Yao, L. A. (1991). The mechanism of arsenic in inhibiting dezincification of brass. *Journal Chinese Society for Corros and Protection*, 11(1), 75–82.

Godish, T. (2004). *Air quality* (4th ed.). Boca Raton: CRC.

Hutzinger, O. (Ed.). (1989). *The handbook of environmental chemistry*. Verlag: Springer.

ISO 8407. (2009). *Corrosion of metals and alloys—removal of corrosion products from corrosion test specimens*. UK: International Organization for Standards.

ISO 8565. (2011). *Metals and alloys—atmospheric corrosion testing—general requirements*. Switzerland: International Organization for Standards.

ISO 9226. (2012). *Corrosion of metals and alloys—corrosivity of atmospheres—determination of corrosion rate of standard specimens for the evaluation of corrosivity*. Switzerland: International Organization for Standards.

Knotkova, D., Boschek, P., & Kreislova, K. (1995). Effect of acidification on atmospheric corrosion of structural metals in Europe. *Water Air Soil Pollution*, 85(4), 2661–2666.

Kucera, V., & Fitz, S. (1996). Direct and indirect air pollution effects on materials including cultural monuments. *Water Air Soil Pollution*, 85(1), 153–165.

Landolt, D. (1993). *Corrosion et chimie de surfaces des métaux 2*. Lausanne: Presse Polytechniques et Universitaires Romandes.

Leidheiser, H., Jr. (1971). *The corrosion of copper, tin, and their alloys*. New York: Wiley.

Maeda, Y., Morioka, J., Tsujino, Y., Satoh, Y., Zhang, X., Mizoguchi, T., & Hatakeyama, S. (2001). Material damage caused by acidic air pollution in East Asia. *Water Air Soil Pollution*, 130(1–4), 141–150.

Mikhailov, A. A., Suloeva, M. N., & Vasilieva, E. G. (1995). Environmental aspects of atmospheric corrosion. *Water Air Soil Pollution*, 85(4), 2673–2678.

Nord, A. G., Tronner, K., & Boyce, A. (2001). Atmospheric bronze and copper corrosion as an environmental indicator. *Water Air Soil Pollution*, 127(1–4), 193–204.

Shreir, L. L. (1963). *Corrosion: Vol. 1, Corrosion of metals and alloys*. New York: Wiley.

Syed, S. (2010). Atmospheric corrosion of carbon steel at marine sites in Saudi Arabia. *Materials and Corrosion*, 61(3), 238–244.

Tzani, C., Varotsos, C., Ferm, M., Christodoulakis, J., Assimakopoulos, M. N., & Efthymiou, C. (2009). Nitric acid and particulate matter measurements at Athens, Greece, in connection with corrosion studies. *Atmospheric Chemistry and Physics*, 9(21), 8309–8316.

- Tzanis, C., Varotsos, C., Christodoulakis, J., Tidblad, J., Ferm, M., Lonescu, A., Lefevre, R.-A., Theodorakopoulou, K., & Kreislova, K. (2011). On the corrosion and soiling effects on materials by air pollution in Athens, Greece. *Atmospheric Chemistry and Physics*, *11*(23), 12039–12048.
- Upham, J. B. (1967). Atmospheric corrosion studies in two metropolitan areas. *Journal Air Pollution Control Association*, *17*(6), 398–402.
- Vargel, C. (2004). *Corrosion of aluminum*. Oxford: Elsevier.
- Wallinder, I. O., & Leygraf, C. (2001). Seasonal variations in corrosion rate and runoff rate of copper roofs in an urban and a rural atmospheric environment. *Corrosion Science*, *43*(12), 2379–2396.
- Wang, D. W., Guo, H., & Chan, C. K. (2012). Measuring ambient acidic ultrafine particles using iron nano-film detectors: method development. *Aerosol Science and Technology*, *46*(5), 521–532.